

2009/2032A

厚生労働科学研究費補助金

医療機器開発推進研究事業

テロメラーゼ依存性蛍光発現ナノバイオ・ウイルス製剤を標識薬剤と  
する高感度リアルタイム微小癌転移イメージング  
システムの開発

(H21-ナノ-一般-008)

平成21年度 総括研究報告書

研究代表者 藤原 俊義

平成22 (2010) 年 5月

# 目 次

I.	総括研究報告 -----	1
	「テロメラーゼ依存性蛍光発現ナノバイオ・ウイルス製剤を標識薬剤と する高感度リアルタイム微小癌転移イメージングシステムの開発」	
II.	研究成果の刊行に関する一覧表 -----	7
III.	研究成果の刊行物・別刷 -----	8

## テロメラーゼ依存性蛍光発現ナノバイオ・ウイルス製剤を標識薬剤とする 高感度リアルタイム微小癌転移イメージングシステムの開発

研究代表者 藤原 俊義

岡山大学病院・遺伝子・細胞治療センター・准教授

### 【研究要旨】

天然に存在する生物由来の蛍光タンパク質は、至適な波長の励起光を吸収することにより強い蛍光を発生し、導入した細胞を生きのままの状態で見ることが可能である。Green Fluorescent Protein (GFP) をはじめとする蛍光タンパク質を用いた分子イメージングは、最先端の生命科学の研究や技術開発には広範囲に利用されているが、医療への応用は未だ研究段階であり、実際にヒトに臨床応用された事例はない。平成17-19年度の厚生労働科学研究費にて、標識薬剤としてテロメラーゼ活性依存性に癌細胞で選択的に増殖してGFP遺伝子を発現するウイルス製剤TelomeScan（開発コード：OBP-401）を作成し、携帯用接触プローブ型蛍光検出装置の有用性を明らかにしてきた。本研究では、新たに鏡視下手術用の高感度蛍光感知機能を付与したビデオスコープを試作し、大動物でその操作性と有用性を評価することで、最近の腹腔鏡・胸腔鏡手術の普及に対応した、より実践的な低侵襲治療の確立を目指す。本年度は、高感度蛍光検出ビデオスコープの試作機を作成し、TelomeScanと同一の蛍光特性を持つ蛍光ビーズをミニブタの胃粘膜下へ注入することでリアルタイムにリンパ流を可視化できることを明らかにした。また、より深部の微小癌組織を高感度に検出するために、組織透過性の高い近赤外蛍光を発生する新たなウイルス標識薬剤の遺伝子改変を行った。

### A. 研究目的

天然に存在する生物由来の蛍光タンパク質は、至適な波長の励起光を吸収することにより強い蛍光を発生し、導入した細胞を生きのままの状態で見ることが可能である。GFP (Green Fluorescent Protein) をはじめとする蛍光タンパク質を用いた分子イメージングは、最先端の生命科学の研究や技術開発には広範囲に利用されているが、医療への応用は未だ研究段階であり、実際にヒトに臨床応用された事例はない。われわれは、テロメラーゼ活性 (hTERT遺伝子発現) に依存して癌細胞で選択的に増殖し細胞死を誘導する改変アデノウイルス製剤Telomelysin（開発コード：OBP-301）を開発し、米国にて臨床試験を行い、その安全性と臨床効果を確認した。このウイルスのゲノム配列は完全に明らかになっており、癌選択的ベクターとして外来遺伝子を搭載することができる。すなわち、蛍光タンパク質をコードする遺伝子を組み込み、癌細胞で選択的に蛍光発現を誘導することができる。

本研究では、テロメラーゼ活性依存性に癌細胞で選択的に増殖してGFP遺伝子を発現するナノバイオ・ウイルス製剤TelomeScan (OBP-401) を標識薬剤とし、鏡視下手術用の高感度蛍光感知ビデオスコープを用いたリアルタイム微小癌転移診断用の外科ナビゲーション・システムを開発する。また、

GFPの蛍光波長より長く、組織透過性の高い近赤外蛍光を発生する新しい蛍光タンパク質遺伝子を搭載した新規ウイルス標識薬剤を開発し、鏡視下手術時における有用性や汎用性をTelomeScanと比較検討する。術前に原発病巣や体腔に投与されたナノバイオ・ウイルス製剤は、微小転移巣で癌細胞に感染・増殖して選択的に蛍光を発生するので、高感度蛍光検出ビデオスコープを用いてリアルタイムにハイビジョン・モニター上で可視化することができる。

平成21年度は、高感度蛍光検出ビデオスコープの試作機を作成し、TelomeScanと同一の蛍光特性を持つ蛍光ビーズを用いた大動物実験を行った。また、近赤外蛍光を発生する新たなウイルス標識薬剤の遺伝子改変を試みた。

### B. 研究方法

#### 1) TelomeScan (OBP-401) の構造と機能

TelomeScanは幼児の「かぜ」症状の原因となるアデノウイルス5型を基本骨格とし、テロメラーゼ構成成分であるhTERT (human telomerase reverse transcriptase) 遺伝子のプロモーターの下流にウイルス増殖に必須のE1AおよびE1B遺伝子がIRES配列で連結して組み込まれている。また、ウイルスゲノムのE3領域に、オワンクラゲ由来のGFP (Green Fluorescent Protein) 蛍光発現遺伝子が挿入されてい

る。TelomeScanは癌細胞で選択的に増殖してGFP蛍光を発するとともに、最終的には細胞死を誘導する。一方、テロメラーゼ活性を持たない正常細胞では、その増殖は抑制され、GFPもみられず、細胞死も生じることはない。

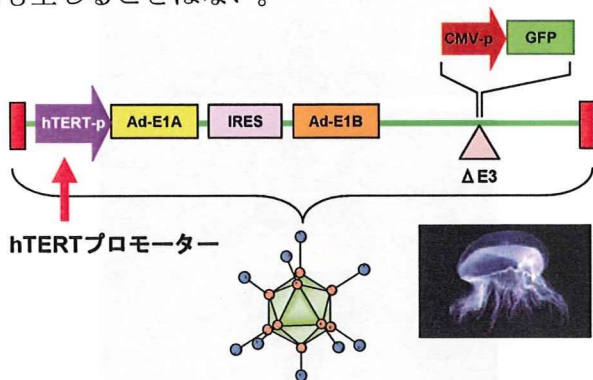


図1 TelomeScanウイルスの構造

## 2) 高感度蛍光検出ビデオスコープ第1号試作機の作成

GFP蛍光を可視化することができる高感度蛍光検出ビデオスコープの第1号機を試作した。明視野モード時は白色光(400~700nm)、蛍光モード時は励起光(460~480nm)を照明光とし、反射光と蛍光をスコープに装着したカメラアダプタで分離して、反射光画像と蛍光画像を同時に表示するシステムとした。明視野モードと蛍光モードは光源で切り替えることができる。

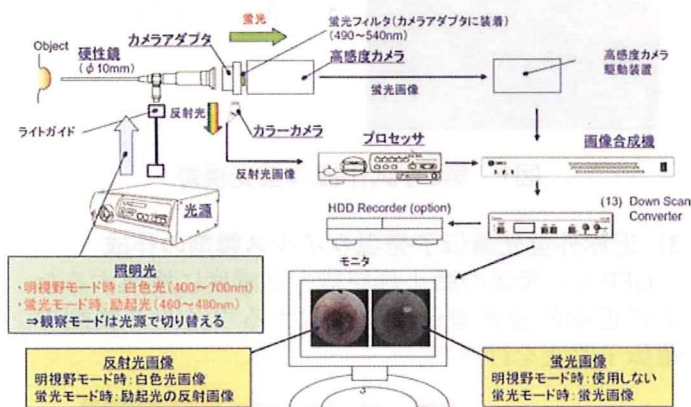


図2 ビデオスコープ第1号試作機のシステム図

## 3) ミニブタを用いた大動物実験

ビデオスコープ試作機を用いて、GFP蛍光が大動物にて検出可能かどうかを検討した。TelomeScanは担癌動物モデルでのみGFP蛍光を発するが、大動物では適した担癌モデルが存在しないため、本実験ではTelomeScanと同一の蛍光特性を持つ蛍光ビーズ(Fluoresbrite蛍光マイクロスフェア、フナコシ株式会社)(50、200、500nm)を使用した。

全身麻酔下にミニブタの下腹部にトロッカーを

挿入し、炭酸ガスにて気腹した後、試作したビデオスコープで腹腔内を観察した。

## 4) 高感度蛍光検出ビデオスコープ第2号試作機の作成

高感度蛍光検出ビデオスコープ第1号試作機の使用経験に基づき、第2号試作機を作成した。カメラヘッドを100~200g程度に小型化し、カメラヘッドのスイッチにて明視野モードと蛍光モードのフィルタ切り替えがワンタッチでできるようにした。また、カメラヘッド部での切り替えに連動して光源フィルタとモニタ表示が切り替わり、明視野と蛍光視野を切り替えて表示するシステムとなっている。

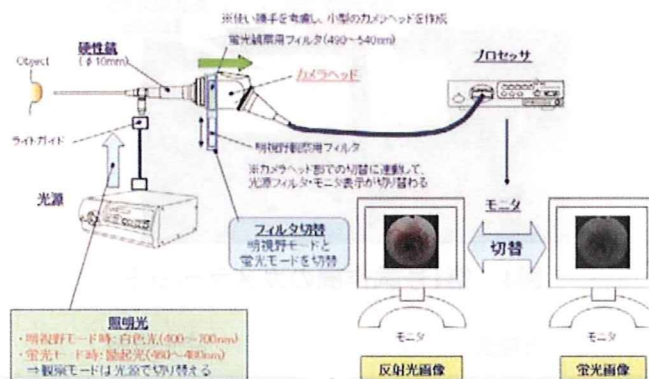


図3 ビデオスコープ第2号試作機のシステム図

## 5) 近赤外蛍光遺伝子発現ウイルス製剤の作成

GFPより深部の微小癌組織を高感度に検出するために、組織透過性の高い近赤外蛍光を発する蛍光タンパク質を搭載した新たなウイルス標識薬剤の作成を試みた。候補遺伝子として、GFPの蛍光波長505nmより長く組織透過性の高い635nmの近赤外蛍光を発するイソギンチャク*Entacmaea quadricolor*由来の新しい蛍光タンパク質Katushka、あるいは蛍光波長610nmの*Anthomedusae*クラゲ由来で光刺激によって活性酸素(reactive oxygen species: ROS)を産生する蛍光タンパク質KillerRedを考えている。

### (倫理面への配慮)

制限増殖型ウイルス製剤を用いる本研究は「大臣確認実験」となるため、「第二種使用等拡散防止措置確認申請書」を作成、学内の担当部署での検討の後に文部科学省に申請し、研究計画実施の承認を得ている。

## C. 研究結果

### 1) 高感度蛍光検出ビデオスコープ第1号試作機による大動物実験

全身麻酔下にミニブタにトロッカー5本を挿入し、臍下部のポートから第1号試作機のビデオスコープを挿入して腹腔内を観察した。次に、経口的に上

部消化管内視鏡を挿入し、胃粘膜下に注射ニードルにて蛍光ビーズ1 mlを注入したところ、腹腔内からの蛍光視野にてリアルタイムに所属リンパ節領域へのリンパ流が可視化できた。しかし、この試作機はカメラヘッドが約1Kgと重く、視野切り替えを光源サイドで行うため、操作性に難点がみられた。

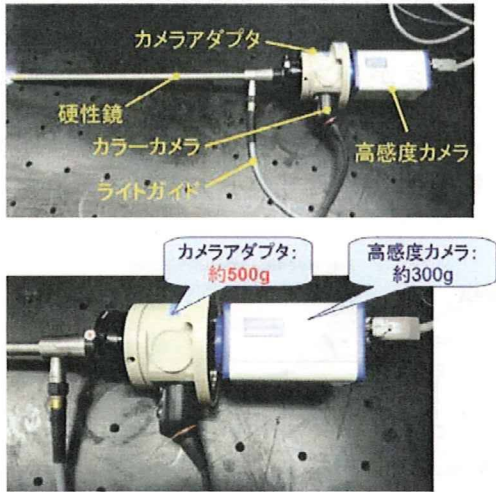


図4 第1号試作機のカメラヘッド

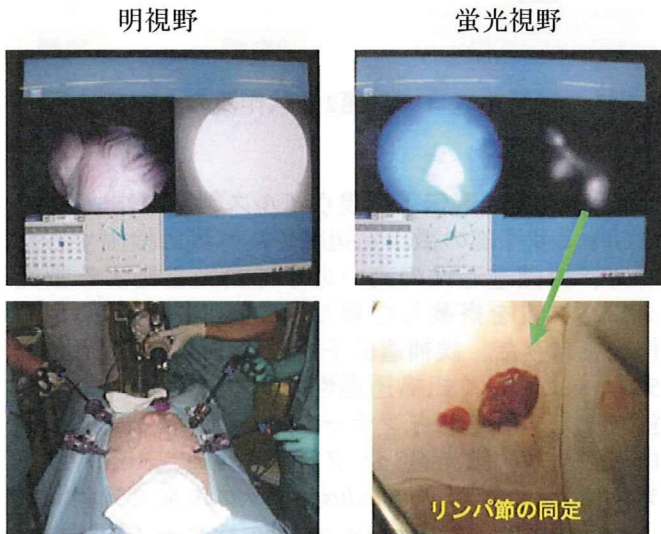


図5 第1号試作機の蛍光視野

## 2) 高感度蛍光検出ビデオスコープ第2号試作機による大動物実験

第1号機での問題点を解決するために、カメラヘッドを小型化し、カメラヘッドのスイッチにて視野モードのフィルタ切り替えができるようにした。また、明視野と蛍光視野を同一モニターで表示するシステムとすることで、視野を動かさずに手術操作が可能となった。小型化によってCCDの感度はやや低下したが、上部消化管内視鏡による胃粘膜下への蛍光ビーズ注入によって、極めて良好にリアルタイムにリンパ流を確認することが可能であった。

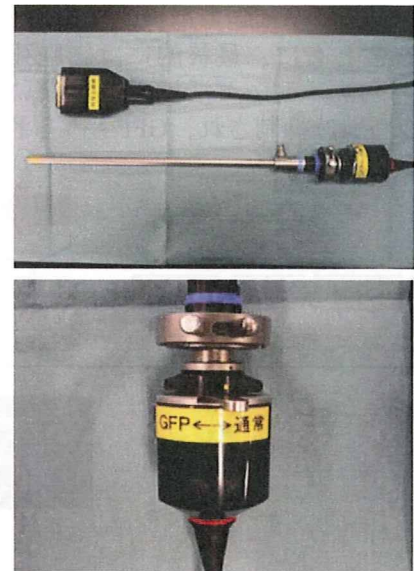


図6 第2号試作機のカメラヘッド

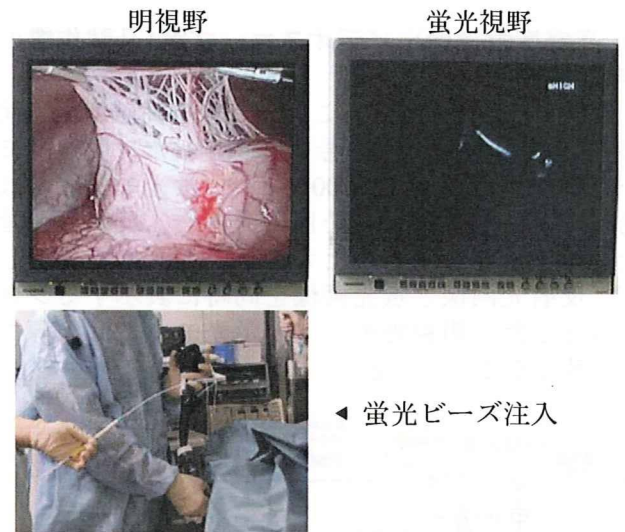


図7 第2号試作機の蛍光視野

## 3) 近赤外蛍光遺伝子発現ウイルス製剤の作成

GFPより深部の微小癌組織を高感度に検出するために近赤外蛍光遺伝子を搭載するウイルス製剤の遺伝子改変を行った。

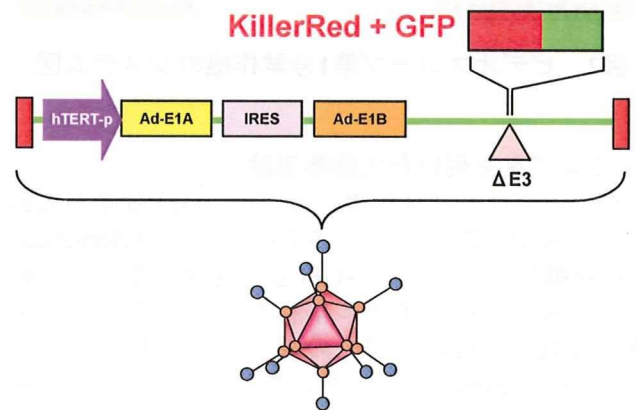


図8 近赤外蛍光遺伝子発現ウイルスの構造

## D. 考察

蛍光タンパク質を用いた *in vivo* 蛍光イメージングは、最先端の生命科学の研究に重要な技術であるが、医療の現場で実用化された事例はまだない。テロメラーゼ活性に反応して増殖する遺伝子改変アデノウイルスは80-100 nmの天然のバイオ・ナノマシンであり、癌細胞で選択的に蛍光遺伝子を発現するために適したベクターと成り得る。投与されたウイルス標識薬剤はリンパ流や血流に乗って拡散し、微小転移病巣で増殖するとともに蛍光発現を生じる。高感度蛍光感知ビデオスコープを組み合わせることで鏡視下手術用外科ナビゲーション・システムの臨床応用が実現すれば、手術中にリアルタイムにリンパ節転移などの微小癌組織を同定することができ、必要最小限の領域を切除する超縮小手術の施行が可能となる。

たとえば早期消化器癌の場合、本技術による診査腹腔鏡や経管腔的内視鏡手術 (NOTES、Natural Orifice Translumenal Endoscopic Surgery) で確実にリンパ節転移や播種がないことを確認できれば、原発巣は内視鏡的粘膜下切開術 (ESD、Endoscopic Submucosal Dissection) のみで切除可能なケースも増えてくる。すなわち、本研究成果によって、外科切除範囲を最小限に留めることで大部分の臓器を温存したり、あるいはリンパ節郭清そのものを省略したりすることができれば、画期的な機能温存が可能となり、治療後の患者の生活の質の著しい向上に貢献することができる。

研究初年度である本年度は、主に検出機器としての高感度蛍光検出装置の試作を行った。GFPと同様の蛍光波長を有する蛍光ビーズの流れをリアルタイムに可視化可能であることが確認でき、今後はウイルス製剤による蛍光発現が検出可能であるかどうかの段階へと進んでいく。また、より深部の微小癌組織を高感度に検出するために、組織透過性の高い近赤外蛍光を発する蛍光タンパク質を搭載した新たなウイルス標識薬剤を作成するとともに、ウイルス製剤の臨床用ロットを製造し、実際の早期胃癌患者における術前投与の臨床研究・臨床試験を目指す。

## E. 結論

GFPの蛍光を可視化することができる高感度蛍光検出ビデオスコープ試作機を作成し、生体内における蛍光ビーズの動態を可視化することで、極めて良好にリアルタイムにリンパ流を確認することができた。

## F. 研究発表

### 1. 論文発表

#### 【英文】

1. Watanabe, Y., Kojima, T., Kagawa, S., Uno, F., Hashimoto, Y., Kyo, S., Mizuguchi, H., Tanaka, N., Kawamura, H., Ichimaru, D., Urata, Y., Fujiwara, T. A novel translational approach for human

- malignant pleural mesothelioma: heparanase-assisted dual virotherapy. *Oncogene*, (in press), 2010.
2. Nemunaitis, J., Tong, A. W., Nemunaitis, M., Senzer, N., Phadke, A. P., Bedell, C., Adams, N., Zhang, Y. A., Maple, P. B., Chen, S., Pappen, B., Burke, J., Ichimaru, D., Urata, Y., Fujiwara, T. A phase I study of telomerase specific replication competent oncolytic adenovirus (Telomelysin) for various solid tumors. *Mol. Ther.*, 18: 429-434, 2010.
3. Kurihara, Y., Watanabe, Y., Onimatsu, H., Kojima, T., Shiota, T., Hatori, M., Liu, D., Kyo, S., Mizuguchi, H., Urata, Y., Shintani, S., Fujiwara, T. Telomerase-specific virotheranostics for human head and neck cancer. *Clin. Cancer Res.*, 15: 2335-2343, 2009.
4. Ikeda, Y., Kojima, T., Kuroda, S., Endo, Y., Sakai, R., Hioki, M., Kishimoto, H., Uno, F., Kagawa, S., Watanabe, Y., Hashimoto, Y., Urata, Y., Tanaka, N., Fujiwara, T. A novel antiangiogenic effect for telomerase-specific virotherapy through host immune system. *J. Immunol.*, 182: 1763-1769, 2009.
5. Liu, D., Kojima, T., Ouchi, M., Kuroda, S., Watanabe, Y., Hashimoto, Y., Onimatsu, H., Urata, Y., Fujiwara, T. Preclinical evaluation of synergistic effect of telomerase-specific oncolytic virotherapy and gemcitabine for human lung cancer. *Mol. Cancer Ther.*, 8: 980-987, 2009.
6. Kishimoto, H., Zhao, M., Hayashi, K., Urata, Y., Tanaka, N., Fujiwara, T., Penman, S., Hoffman, R. M. In vivo internal tumor illumination by telomerase-dependent adenoviral GFP for precise surgical navigation. *Proc. Natl. Acad. Sci. U S A*, 106: 14514-14517, 2009.
7. Kojima, T., Hashimoto, Y., Watanabe, Y., Kagawa, S., Uno, F., Kuroda, S., Tazawa, H., Kyo, S., Mizuguchi, H., Urata, Y., Tanaka, N., Fujiwara, T. A simple biological imaging system for detecting viable human circulating tumor cells. *J. Clin. Invest.*, 119: 3172-3181, 2009.
8. Kishimoto, H., Urata, Y., Tanaka, N., Fujiwara, T., Hoffman, R. M. Selective metastatic tumor labeling with green fluorescent protein and killing by systemic administration of telomerase-dependent adenoviruses. *Mol. Cancer Ther.*, 8: 3001-3008, 2009.
9. Ouchi, M., Kawamura, H., Urata, Y., Fujiwara, T. Antiviral activity of cidofovir against telomerase-specific replication-selective oncolytic adenovirus, OBP-301 (Telomelysin). *Invest. New Drugs*, 27: 241-245, 2009.
10. Nakajima, O., Matsunaga, A., Ichimaru, D., Urata, Y., Fujiwara, T., Kawakami, K. Telomerase-specific virotherapy in an animal model of human head and neck cancer. *Mol. Cancer Ther.*, 8: 171-177, 2009.
11. Maida, Y., Kyo, S., Sakaguchi, J., Mizumoto, Y., Hashimoto, M., Mori, N., Ikoma, T., Nakamura, M.,

- Takakura, M., Urata, Y., Fujiwara, T., Inoue, M. Diagnostic potential and limitation of imaging cancer cells in cytological samples using telomerase-specific replicative adenovirus. *Int. J. Oncol.*, 34: 1549-1556, 2009.
12. Takakura, M., Nakamura, M., Kyo, S., Hashimoto, M., Mori, N., Ikoma, T., Mizumoto, Y., Fujiwara, T., Urata, Y., Inoue, M. Intraperitoneal administration of telomerase-specific oncolytic adenovirus sensitizes ovarian cancer cells to cisplatin and affects survival in a xenograft model with peritoneal dissemination. *Cancer Gene Ther.*, (Epub ahead of print), 2009.
  13. Nakajima, O., Ichimaru, D., Urata, Y., Fujiwara, T., Horibe, T., Kohno, M., Kawakami, K. Use of telomelysin (OBP-301) in mouse xenografts of human head and neck cancer. *Oncol. Rep.*, 22: 1039-1043, 2009.
  14. Fujiwara, T. Telomerase-specific virotherapy for human squamous cell carcinoma. *Expert Opin. Biol. Th.*, 9: 321-329, 2009.
  15. Fujiwara, T., Urata, Y., Tanaka, N. Telomerase-specific gene and vector-based therapies for human cancer. In “*Telomeres and Telomerase in Cancer*” (Hiyama, K., ed.), pp293-312, Humana Press, New York, USA, 2009.

#### 【邦文】

1. 藤原俊義、田中紀章：遺伝子治療・ウイルス治療。 *日本臨床増刊号「がん薬物療法学」* 67: 306-313, 2009.
2. 藤原俊義：遺伝子治療の現状と展望。 *呼吸器科* 15: 139-146, 2009.
3. 藤原俊義：固形癌に対するウイルス療法。 *癌と化学療法* 36: 703-709, 2009.
4. 藤原俊義：遺伝子治療。 「*がん化学療法・分子標的治療 update*」 (西條長宏、西尾和人、編集) pp281-288、中外医学社、2009.

#### 2. 学会発表

##### 【国際学会】

1. Fujiwara, T. Telomerase-specific oncolytic virotherapy for human cancer. *Japan-Denmark Joint Workshop “Molecular Cancer Research” [invited]*, Tokyo, 2009.
2. Fujiwara, T., Yano, S. A novel telomerase-specific oncolytic virotherapy targeting cancer stem cells. *The 8<sup>th</sup> Japan-China Joint Conference for Cancer Research “Cancer Stem Cell, microRNA, and Cancer Immunology” [invited]*, Osaka, 2009.
3. Yano, S., Hashimoto, Y., Kuroda, S., Kojima, T., Uno, F., Tazawa, H., Kagawa, S., Urata, Y., Tanaka, N., Fujiwara, T. Telomerase-specific oncolytic virotherapy purging cancer stem cells. *2009 Annual Meeting of the American Association for Cancer Research*, 2009.
4. Tazawa, H., Hashimoto, Y., Kuroda, S., Urata, Y., Fujiwara, T. Preclinical study of telomerase-

selective oncolytic adenovirus (OBP-301) in combination with chemotherapeutic agents. *2009 Annual Meeting of the American Association for Cancer Research*, 2009.

5. Yamasaki, Y., Onimatsu, H., Hashimoto, Y., Kojima, T., Tazawa, H., Kagawa, S., Mizuguchi, H., Urata, Y., Tanaka, N., Fujiwara, T. Telomerase-specific oncolytic adenovirus armed with wild-type p53 gene (CGCT-04) efficiently induces apoptosis in human cancer cells. *2009 Annual Meeting of the American Association for Cancer Research*, 2009.
6. Hashimoto, Y., Kojima, T., Uno, F., Kagawa, S., Watanabe, Y., Kuroda, S., Urata, Y., Tanaka, N., Fujiwara, T. Biological imaging system to detect viable circulating tumor cells is useful for monitoring the efficacy of treatment in cancer patients. *2009 Annual Meeting of the American Association for Cancer Research*, 2009.
7. Kuroda, S., Fujiwara, T., Tazawa, H., Uno, F., Kagawa, S., Hashimoto, Y., Ouchi, M., Urata, Y., Tanaka, N., Fujiwara, T. Telomerase-specific oncolytic adenovirus mediates molecular sensitization to ionizing radiation in human cancer cells through E1B55kDa expression. *2009 Annual Meeting of the American Association for Cancer Research*, 2009.
8. Kojima, T., Hashimoto, Y., Kuroda, S., Yamasaki, Y., Yano, S., Tazawa, H., Uno, F., Kagawa, S., Urata, Y., Tanaka, N., Fujiwara, T. Biological purging of lymph node metastasis of gastrointestinal cancer by telomerase-specific virotherapy. *2009 Annual Meeting of the American Association for Cancer Research*, 2009.
9. Kurihara, Y., Kojima, T., Shirota, T., Hatori, M., Urata, Y., Fujiwara, T., Shintani, S. Preclinical evaluation of telomerase-specific virotheranostics for human head and neck cancer. *2009 Annual Meeting of the American Association for Cancer Research*, 2009.
10. Kishimoto, H., Urata, Y., Fujiwara, T., Bouvet, M., Hoffman, R. M. Systemic tumor targeting by a telomerase-specific replicating adenovirus (OBP-301) results in inhibition of metastasis. *2009 Annual Meeting of the American Association for Cancer Research*, 2009.

##### 【国内学会】

1. 香川俊輔、宇野太、橋本悠里、浦田泰生、田中紀章、藤原俊義：テロメラーゼ活性を標的とするウイルス製剤 OBP-301 の臨床応用：固形腫瘍に対する第 I 相臨床試験。 *第 109 回日本外科学会定期学術集会 (シンポジウム)*、2009.
2. 藤原俊義：テロメラーゼ活性を標的とするアデノウイルス製剤の癌診断・治療への応用。 *第 25 回日本 DDS 学会 (シンポジウム)*、2009.
3. 藤原俊義：テロメラーゼ特異的腫瘍融解アデノウイルスによる放射線感受性増強とその分

- 子機構の解析. **第39回放射線による制癌シンポジウム (シンポジウム)**、2009.
4. 藤原俊義、浦田泰生、田中紀章：悪性腫瘍に対するテロメラーゼ特異的腫瘍融解ウイルス療法. **第68回日本癌学会学術総会**、2009.
  5. 香川俊輔、黒田新士、宇野太、田澤大、浦田泰生、藤原俊義：肺癌に対する分子療法. **第68回日本癌学会学術総会 (シンポジウム)**、2009.
  6. Yamasaki, Y., Onimatsu, H., Hashimoto, Y., Kojima, T., Tazawa, H., Kagawa, S., Mizuguchi, H., Urata, Y., Tanaka, N., Fujiwara, T. Telomerase-specific oncolytic adenovirus armed with wild-type p53 gene (CGCT-04) efficiently induces apoptosis in human cancer cells. **第15回日本遺伝子治療学会**、2009.
  7. Tazawa, H., Hashimoto, Y., Kuroda, S., Urata, Y., Fujiwara, T. Preclinical study of telomerase-selective oncolytic adenovirus (OBP-301) in combination with chemotherapeutic agent and radiation. **第15回日本遺伝子治療学会**、2009.
  8. 矢野修也、橋本悠里、田澤大、山崎泰源、宇野太、香川俊輔、浦田泰生、田中紀章、藤原俊義：テロメラーゼ特異的腫瘍融解ウイルスはより多く複製することで胃癌幹細胞を効率的に破壊する. **第68回日本癌学会学術総会**、2009.
  9. 田澤大、矢野修也、吉田亮介、浦田泰生、藤原俊義：テロメラーゼ依存性腫瘍融解ウイルスの細胞障害に伴うマイクロRNA-7の発現誘導はオートファジー細胞死を引き起こす. **第68回日本癌学会学術総会**、2009.
  10. 高倉正博、京哲、中村充宏、橋本学、森紀子、水本泰成、生駒友美、藤原俊義、井上正樹：腫瘍特異的増殖性アデノウイルスの薬剤耐性卵巣癌への効果の検討. **第68回日本癌学会学術総会**、2009.
  11. 大内正明、永井勝幸、浦田泰生、藤原俊義：テロメラーゼ依存性腫瘍融解ウイルス製剤と温熱療法の併用. **第68回日本癌学会学術総会**、2009.
  12. 橋本悠里、児島亨、宇野太、香川俊輔、渡邊雄一、黒田新士、浦田泰生、田中紀章、藤原俊義：テロメラーゼ依存的制限増殖型 GFP 発現アデノウイルスによる末梢血中ヒト循環がん細胞の検出. **第68回日本癌学会学術総会**、2009.
  13. 吉田亮介、田澤大、山崎泰源、矢野修也、宇野太、香川俊輔、橋本悠里、大内正明、藤原俊義：リンパ節可視化のための新しい体内光学イメージングシステムのブタにおける前臨床的評価. **第68回日本癌学会学術総会**、2009.
  14. 川島寛之、生越章、藤原俊義、浦田泰生：テロメラーゼ活性を標的とした骨肉腫に対するウイルス療法. **第68回日本癌学会学術総会**、2009.
  15. 山崎泰源、鬼松秀樹、橋本悠里、田澤大、香川俊輔、水口裕之、浦田泰生、田中紀章、藤原俊義：テロメラーゼ特異的腫瘍融解アデノウイルスによる p53 の過剰発現は AdE1A による p21 不活化によりアポトーシスを誘導する. **第68回日本癌学会学術総会**、2009.



研究成果の刊行に関する一覧表

雑誌

発表者氏名	論文タイトル名	発表誌名	巻号	ページ	出版年
Kurihara, Y., Watanabe, Y., Onimatsu, H., Kojima, T., Shiota, T., Hatori, M., Liu, D., Kyo, S., Mizuguchi, H., Urata, Y., Shintani, S., Fujiwara, T.	Telomerase-specific virotheranostics for human head and neck cancer.	<b>Clinical Cancer Research</b>	15	2335-2343	2009
Ouchi, M., Kawamura, H., Urata, Y., Fujiwara, T.	Antiviral activity of cidofovir against telomerase-specific replication-selective oncolytic adenovirus, OBP-301 (Telomelysin).	<b>Investigational New Drugs</b>	27	241-245	2009
Liu, D., Kojima, T., Ouchi, M., Kuroda, S., Watanabe, Y., Hashimoto, Y., Onimatsu, H., Urata, Y., Fujiwara, T.	Preclinical evaluation of synergistic effect of telomerase-specific oncolytic virotherapy and gemcitabine for human lung cancer.	<b>Molecular Cancer Therapeutics</b>	8	980-987	2009
Kishimoto, H., Zhao, M., Hayashi, K., Urata, Y., Tanaka, N., Fujiwara, T., Penman, S., Hoffman, R. M.	In vivo internal tumor illumination by telomerase-dependent adenoviral GFP for precise surgical navigation.	<b>Proceedings of the National Academy of Sciences of the United States of America</b>	106	14514-14517	2009
Kojima, T., Hashimoto, Y., Watanabe, Y., Kagawa, S., Uno, F., Kuroda, S., Tazawa, H., Kyo, S., Mizuguchi, H., Urata, Y., Tanaka, N., Fujiwara, T.	A simple biological imaging system for detecting viable human circulating tumor cells.	<b>Journal of Clinical Investigation</b>	119	3172-3181	2009
Kishimoto, H., Urata, Y., Tanaka, N., Fujiwara, T., Hoffman, R. M.	Selective metastatic tumor labeling with green fluorescent protein and killing by systemic administration of telomerase-dependent adenoviruses.	<b>Molecular Cancer Therapeutics</b>	8	3001-3008	2009
Nemunaitis, J., Tong, A. W., Nemunaitis, M., Senzer, N., Phadke, A. P., Bedell, C., Adams, N., Zhang, Y. A., Maple, P. B., Chen, S., Pappen, B., Burke, J., Ichimaru, D., Urata, Y., Fujiwara, T.	A phase I study of telomerase-specific replication competent oncolytic adenovirus (Telomelysin) for various solid tumors.	<b>Molecular Therapy</b>	18	429-434	2010

## Telomerase-Specific Virotheranostics for Human Head and Neck Cancer

Yuji Kurihara,<sup>1</sup> Yuichi Watanabe,<sup>2,3</sup> Hideki Onimatsu,<sup>2</sup> Toru Kojima,<sup>4</sup> Tatsuo Shirota,<sup>1</sup> Masashi Hatori,<sup>1</sup> Dong Liu,<sup>5</sup> Satoru Kyo,<sup>6</sup> Hiroyuki Mizuguchi,<sup>7</sup> Yasuo Urata,<sup>2</sup> Satoru Shintani,<sup>1</sup> and Toshiyoshi Fujiwara<sup>3,4</sup>

**Abstract Purpose:** Long-term outcomes of patients with squamous cell carcinoma of the head and neck (SCCHN) remain unsatisfactory despite advances in combination of treatment modalities. SCCHN is characterized by locoregional spread and it is clinically accessible, making it an attractive target for intratumoral biological therapies.

**Experimental Design:** OBP-301 is a type 5 adenovirus that contains the replication cassette in which the human telomerase reverse transcriptase promoter drives expression of the *E1* genes. OBP-401 contained the replication cassette and the green fluorescent protein (*GFP*) gene. The antitumor effects of OBP-301 were evaluated *in vitro* by the sodium 30-[1-(phenylaminocarbonyl)-3,4-tetrazolium]-bis(4-methoxy-6-nitro)benzene sulfonic acid hydrate assay and *in vivo* in an orthotopic xenograft model. Virus spread into the lymphatics was also orthotopically assessed by using OBP-401.

**Results:** Intratumoral injection of OBP-301 resulted in the shrinkage of human SCCHN tumors orthotopically implanted into the tongues of BALB/c *nu/nu* mice and significantly recovered weight loss by enabling oral ingestion. The levels of GFP expression following *ex vivo* infection of OBP-401 may be of value as a positive predictive marker for the outcome of telomerase-specific virotherapy. Moreover, whole-body fluorescent imaging revealed that intratumorally injected OBP-401 could visualize the metastatic lymph nodes, indicating the ability of the virus to traffic to the regional lymphatic area and to selectively replicate in neoplastic lesions, resulting in GFP expression and cell death in metastatic lymph nodes.

**Conclusions:** These results illustrate the potential of telomerase-specific oncolytic viruses for a novel therapeutic and diagnostic approach, termed theranostics, for human SCCHN.

Cancer remains a leading cause of death worldwide despite improvements in diagnostic techniques and clinical management (1, 2). An estimated 500,000 patients worldwide are diagnosed with squamous cell carcinoma of the head and neck

(SCCHN) annually. This aggressive epithelial malignancy is associated with a high mortality rate and severe morbidity among the long-term survivors (3). Current treatment strategies for advanced SCCHN include surgical resection, radiation, and cytotoxic chemotherapy. Although a combination of these modalities can improve survival, most patients eventually experience disease progression that leads to death; disease progression is often the result of intrinsic or acquired resistance to treatment (4, 5). A lack of specificity for tumor cells is the primary limitation of radiotherapy and chemotherapy. To improve the therapeutic index, there is a need for anticancer agents that selectively target only tumor cells and spare normal cells.

Replication-selective tumor-specific viruses present a novel approach for cancer treatment (6, 7). We reported previously that telomerase-specific replication-competent adenovirus (OBP-301, Telomelysin), in which the human telomerase reverse transcriptase (hTERT) promoter element drives the expression of *E1A* and *E1B* genes linked with an IRES, induced selective E1 expression, and efficiently killed human cancer cells but not normal cells (8–10). We also found that intratumoral injection of telomerase-specific replication-selective adenovirus expressing the green fluorescent protein (*GFP*) gene (OBP-401, TelomeScan) causes viral spread into the regional lymphatic area with subsequent selective replication in

**Authors' Affiliations:** <sup>1</sup>Department of Oral and Maxillofacial Surgery, School of Dentistry, Showa University and <sup>2</sup>Oncolys BioPharma, Inc., Tokyo, Japan; <sup>3</sup>Center for Gene and Cell Therapy, Okayama University Hospital and <sup>4</sup>Division of Surgical Oncology, Department of Surgery, Okayama University Graduate School of Medicine, Dentistry and Pharmaceutical Sciences, Okayama, Japan; <sup>5</sup>Research Center of Lung Cancer, Shanghai Pulmonary Hospital, Shanghai, China; <sup>6</sup>Department of Obstetrics and Gynecology, Kanazawa University School of Medicine, Kanazawa, Japan; and <sup>7</sup>Department of Biochemistry and Molecular Biology, Graduate School of Pharmaceutical Sciences, Osaka University, Osaka, Japan

Received 10/22/08; revised 12/17/08; accepted 12/31/08; published OnlineFirst 3/24/09.

**Grant support:** Grants-in-Aid from the Ministry of Education, Science, and Culture, Japan (T. Fujiwara), and Grants from the Ministry of Health and Welfare, Japan (T. Fujiwara).

The costs of publication of this article were defrayed in part by the payment of page charges. This article must therefore be hereby marked *advertisement* in accordance with 18 U.S.C. Section 1734 solely to indicate this fact.

**Note:** Supplementary data for this article are available at Clinical Cancer Research Online (<http://clincancerres.aacrjournals.org/>).

**Requests for reprints:** Toshiyoshi Fujiwara, Center for Gene and Cell Therapy, Okayama University Hospital, 2-5-1 Shikata-cho, Okayama 700-8558, Japan. Phone: 81-86-235-7997; Fax: 81-86-235-7884; E-mail: toshi\_f@md.okayama-u.ac.jp.

© 2009 American Association for Cancer Research.

doi:10.1158/1078-0432.CCR-08-2690

### Translational Relevance

Despite new therapeutic modalities, long-term outcomes of patients with squamous cell carcinoma of the head and neck (SCCHN) remain unsatisfactory. Thus, the development of efficient treatment methods to enable the reduction of tumors in these patients is clearly imperative. Tumor-targeted oncolytic viruses have the potential to selectively infect target tumor cells, multiply, and cause cell death and release of viral particles, leading to the spread of viral-mediated antitumor effects. We developed a telomerase-specific oncolytic adenovirus OBP-301 (Telomelysin) as well as OBP-401 – expressing *GFP* gene (TelomeScan). Our data showed that telomerase-specific oncolytic viruses can be effective to kill human SCCHN cells *in vitro* and *in vivo* as well as to identify the patients who will likely benefit from virotherapy, suggesting that an oncolytic virus-based approach exhibited desirable features of a novel “virotheranostics,” the combination of a diagnostic assay with a therapeutic entity for human SCCHN. This is a preclinical study for the future clinical trials.

metastatic lymph nodes in *nu/nu* mice (11). Although up to 25% of patients with SCCHN develop distant metastasis to the lung, liver, or bone, lymph node metastases are more common in SCCHN patients (12); therefore, locoregional disease control with telomerase-specific oncolytic viruses may be a novel therapeutic strategy that is clinically applicable for the treatment of human SCCHN.

In the present study, we explore the therapeutic as well as diagnostic ability of telomerase-specific oncolytic viruses *in vitro* and *in vivo*. To this end, we adopted an orthotopic head and neck cancer xenograft model by inoculating human SCCHN cells into the tongues of *nu/nu* mice; this model resembles human SCCHN in a number of biological properties (13).

### Materials and Methods

**Cell lines and cell culture.** The human oral squamous carcinoma cell lines SAS-L, SCC-4, SCC-9, HSC-2, HSC-3, and HSC-4 were maintained *in vitro* as monolayers in DMEM supplemented with 10% heat-inactivated fetal bovine serum, 100 units/mL penicillin, and 100 mg/mL streptomycin (complete medium). The human non-small-cell lung cancer cell line H460 and the human esophageal cancer cell line TE8 were routinely propagated in monolayer culture in RPMI 1640 supplemented with 10% fetal bovine serum. The normal human lung diploid fibroblast cell line WI38 (JCRB0518) was obtained from the Health Science Research Resources Bank (Osaka, Japan) and grown in Eagle's MEM with 10% fetal bovine serum. The normal human lung fibroblast NHLF (TaKaRa Biomedicals) and the normal human embryonic lung fibroblast MRC-5 (RIKEN BioResource Center) were cultured according to the vendors' specifications.

**Adenoviruses.** The recombinant replication-selective, tumor-specific adenovirus vector OBP-301 (Telomelysin), in which the hTERT promoter element drives the expression of *E1A* and *E1B* genes linked with an IRES, was previously constructed and characterized (8–10). OBP-401 is a telomerase-specific replication-competent adenovirus variant with the replication cassette, and *GFP* gene under the control of the cytomegalovirus promoter was inserted into the E3 region for

monitoring viral replication (11, 14). The viruses were purified by ultracentrifugation in cesium chloride step gradients, their titers were determined by a plaque-forming assay using 293 cells, and they were stored at -80°C.

**Cell viability assay.** An sodium 30-[1-(phenylaminocarbonyl)-3,4-tetrazolium]-bis(4-methoxy-6-nitro)benzene sulfonic acid hydrate (XTT) assay was done to assess the viability of tumor cells. Human SCCHN cells (1,000 per well) were seeded onto 96-well plates 18 to 20 h before viral infection. Cells were then infected with OBP-301 at a multiplicity of infection (MOI) of 1, 10, 50, and 100 plaque-forming units (pfu) per cell. Cell viability was determined at the indicated time points by using a Cell Proliferation Kit II (Roche Molecular Biochemicals) according to the protocol provided by the manufacturer.

**Fluorescence microplate reader.** Cells were infected with OBP-401 at the indicated MOI values in a 96-well black-bottomed culture plate and further incubated for the indicated time periods. GFP fluorescence was measured by using a fluorescence microplate reader (DS Pharma Biomedical) with excitation/emission at 485 nm/528 nm.

**Animal experiments.** SAS-L and HSC-3 human oral squamous cell carcinoma cells were harvested and suspended at a concentration of  $5 \times 10^6$ /mL in the medium. To generate an orthotopic head and neck cancer model, 6-wk-old female BALB/c *nu/nu* mice were anesthetized and injected directly with 20  $\mu$ L of cell suspension at a density of  $10^5$  cells. The cells were injected into the right lateral border of the tongue with a 27-gauge needle. When the tumor grew to 2 to 3 mm in diameter ~5 to 7 days later, 20  $\mu$ L of solution containing  $1 \times 10^8$  pfu of OBP-301, OBP-401, or PBS were injected into the tumor. The perpendicular diameter of each tumor was measured every 3 d, and tumor volume was calculated by using the following formula: tumor volume ( $\text{mm}^3$ ) =  $a \times b^2 \times 0.5$ , where  $a$  is the longest diameter,  $b$  is the shortest diameter, and 0.5 is a constant to calculate the volume of an ellipsoid. The body weights of mice were monitored and recorded. The experimental protocol was approved by the Ethics Review Committee for Animal Experimentation of Okayama University.

**In vivo fluorescence imaging.** *In vivo* GFP fluorescence imaging was acquired by illuminating the animal with a Xenon 150-W lamp. The reemitted fluorescence was collected through a long-pass filter on a Hamamatsu C5810 3-chip color charge-coupled device camera (Hamamatsu Photonics Systems). High-resolution image acquisition was accomplished by using an EPSON PC. Images were processed for contrast and brightness with the use of Adobe Photoshop 4.0.1J software (Adobe). A fluorescence stereomicroscope (SZX7; Olympus) was also used to visualize GFP-positive tissues.

**Statistical analysis.** The statistical significance of the differences in the *in vitro* and *in vivo* antitumor effects of viruses was determined by using the Student's *t* test (two-tailed). The antitumor effect viruses on orthotopically implanted tumors in nude mice were assessed by plotting survival curves according to the Kaplan-Meier method. *P* values <0.05 were considered statistically significant.

### Results

**In vitro cytopathic efficacy of OBP-301 on human SCCHN cell lines.** We examined the cytopathic effect of OBP-301, which is an attenuated adenovirus in which the hTERT promoter element drives expression of *E1A* and *E1B* genes linked with an internal ribosome entry site (IRES; Fig. 1A), on various human SCCHN cell lines by the XTT cell viability assay. OBP-301 infection induced cell death in human SCCHN cells in a dose-dependent manner; the sensitivity, however, varied among different cell lines (Fig. 1B). The ID<sub>50</sub> values calculated from the dose-response curves confirmed that SAS-L cells could be efficiently killed by OBP-301 at an multiplicity of infection (MOI) of <150 (ID<sub>50</sub> = 148), whereas HSC-3 cells were less sensitive to OBP-301 (ID<sub>50</sub> = 500; Fig. 1C).

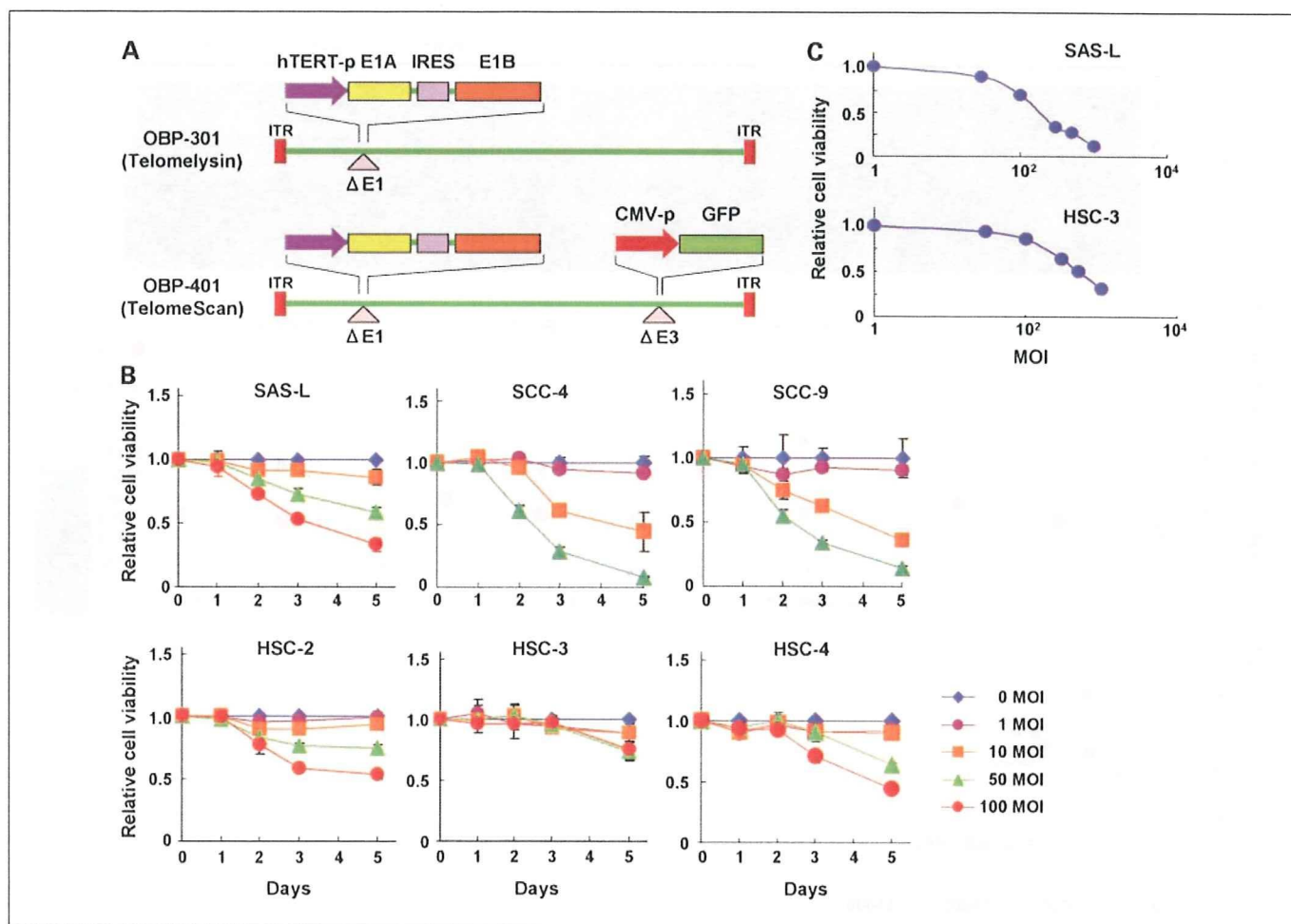


**Fig. 1.** Schematic DNA structures of telomerase-specific viruses and selective cytopathic effect in human SCCHN cell lines *in vitro*. **A**, OBP-301 is a telomerase-specific replication-competent adenovirus containing the hTERT promoter sequence inserted into the adenovirus genome to drive transcription of the E1A and E1B bicistronic cassette linked by the IRES. OBP-401 is a variant of OBP-301, in which the GFP gene is inserted under the cytomegalovirus (CMV) promoter into the E3 region for monitoring viral replication. **B**, human SCCHN cell lines were infected with OBP-301 at the indicated MOI values, and surviving cells were quantitated over 5 d by the XTT assay. The cell viability of mock-treated cells on day 0 was considered 1.0, and the relative cell viability was calculated. Points, mean of triplicate experiments; bars, SD. **C**, effects of various concentrations of OBP-301 on SAS-L and HSC-3 cells assessed 5 d after the XTT assay. Results are expressed as the relative cell viability of untreated control cells.

To confirm the specificity of telomerase activity in human SCCHN cells, we next measured the expression of *hTERT* mRNA in a panel of human SCCHN cell lines and normal cell lines by using a real-time reverse transcription-PCR method. Although the levels of expression varied widely, all SCCHN cell lines expressed detectable levels of *hTERT* mRNA, whereas human fibroblast cells such as NHEL and WI38 were negative for *hTERT* expression (Supplementary Fig. S1A). We also examined the expression levels of coxsackievirus and adenovirus receptor on the cell surface of each type of cell by flow cytometric analysis. Apparent amounts of coxsackievirus and adenovirus receptor expression were detected on SAS-L and HSC-3 human SCCHN cells (Supplementary Fig. S1B).

To assess whether viral replication was restricted to tumor cells, we next examined the replication ability of OBP-301 by measuring the relative amounts of E1A DNA. SAS-L human SCCHN cells and MRC-5 human fibroblasts were harvested at indicated time points over 72 h after infection with OBP-301 and subjected to quantitative real-time PCR analysis. The ratios were normalized by dividing the value of cells obtained 2 h after viral infection. OBP-301 replicated 3 to 4 logs within 48 h after

infection; the viral replication, however, was attenuated up to 2 logs in normal MRC-5 cells (Supplementary Fig. S2).

The response of tumor cells to DNA-damaging stimuli such as chemotherapeutic drugs and ionizing radiation is predetermined by the functional status of their *p53* gene (15); however, the *p53* status of human SCCHN cell lines (wild-type *p53* [SAS-L], mutant *p53* [SCC-4, HSC-2, HSC-3, HSC-4], and deleted *p53* [SCC-9]) is not related to their sensitivity to OBP-301. Indeed, OBP-301 similarly killed parental SAS-L cells and cells stably transfected with the mutant *p53* gene (Supplementary Fig. S3), suggesting that OBP-301 induces cell death in a *p53*-independent manner.

**Selective replication of OBP-401 in human SCCHN cell lines *in vitro*.** OBP-401 is a genetically engineered adenovirus that expresses GFP under the control of the cytomegalovirus promoter at the deleted E3 region of OBP-301 (Fig. 1A). To determine whether OBP-401 replication is associated with selective GFP expression in human SCCHN cells, cells were analyzed and recorded by using a time-lapse fluorescent microscope after OBP-401 infection. Representative images at the indicated time points are shown (Fig. 2A). SAS-L-

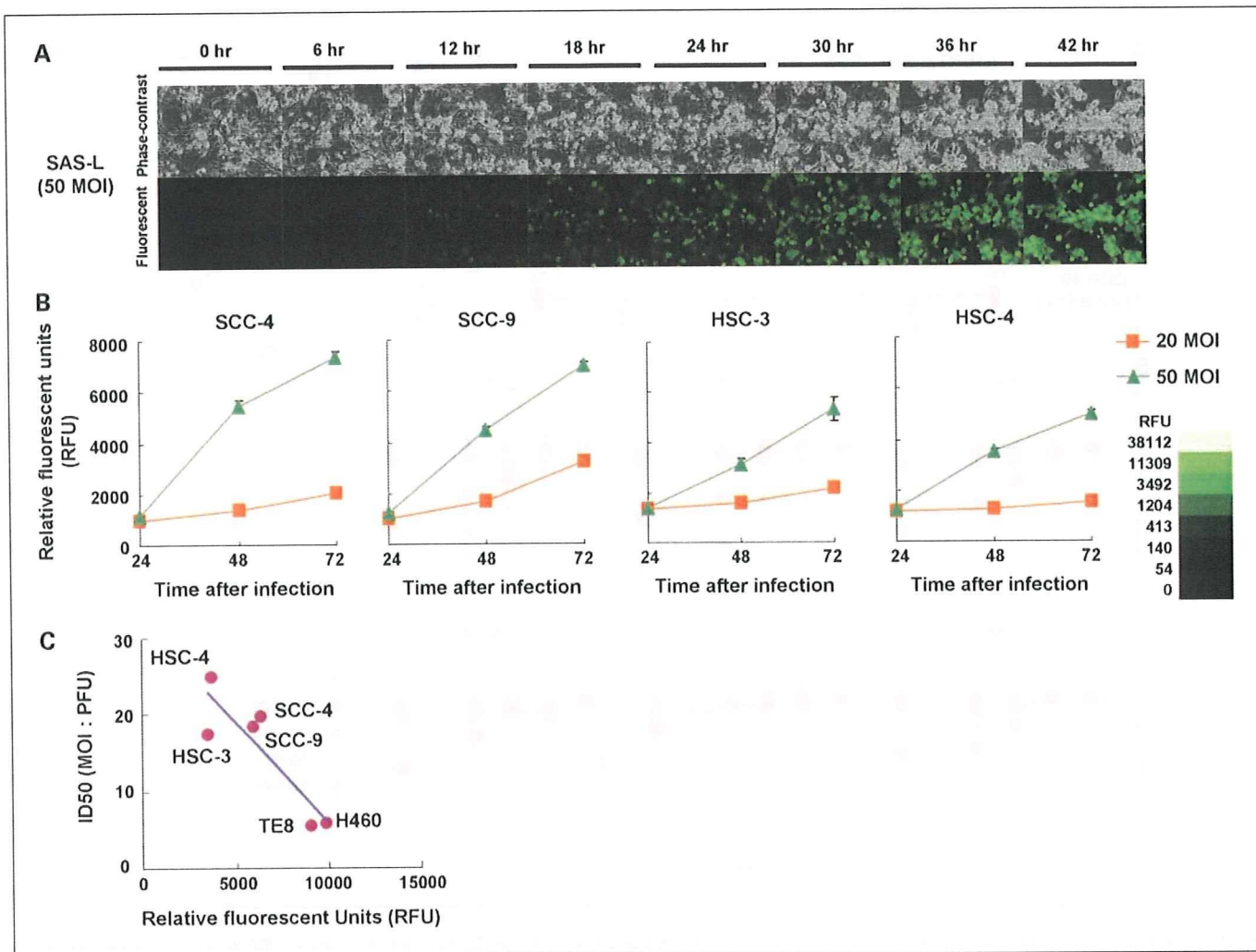


Fig. 2. Selective visualization of human SCCHN cells *in vitro* by OBP-401. **A**, time-lapse images of SAS-L cells were recorded for 42 h after OBP-401 infection at a MOI of 50. Representative images taken at the indicated time points show cell morphology by phase-contrast microscopy (*top*) and GFP expression under fluorescence microscopy (*bottom*). Magnification,  $\times 200$ . **B**, quantitative assessment of GFP labeling by OBP-401 in human SCCHN cell lines. Cells were infected with OBP-401 at the indicated MOI values, and GFP fluorescence was measured over 72 h by the fluorescence microplate reader. The intensity of green fluorescence was evaluated based on the brightness determinations used as relative fluorescence units (RFU). The relative fluorescence unit and time after infection were plotted on the ordinate and abscissa, respectively. A green color calibration bar for the indicated relative fluorescence unit is shown on the right. **C**, relationship between GFP fluorescence after OBP-401 infection and ID<sub>50</sub> values after OBP-301 infection in human cancer cell lines, including SCCHN cells. Relative GFP fluorescence was measured by the fluorescence microplate reader 72 h after OBP-401 infection at a MOI of 50. The ID<sub>50</sub> values of OBP-301 on cell viability at 5 d after infection were calculated and expressed as ID<sub>50</sub> values. The slope represents the inverse correlation between these two factors ( $R^2 = 0.7839$ ).

human SCCHN cells expressed bright GFP fluorescence as early as 12 h after OBP-401 infection at a MOI of 50. The fluorescence intensity gradually increased in a dose-dependent manner, followed by rapid cell death due to the cytopathic effect of OBP-401, as evidenced by floating, highly light-refractile cells under phase-contrast photomicrographs.

We also quantified GFP expression in human SCCHN cells following OBP-401 infection by using a fluorescence plate reader. Relative expression levels of GFP gradually increased in a dose-dependent manner (Fig. 2B). Moreover, we found an apparent inverse correlation between relative GFP expression at 72 h after OBP-401 infection and the ID<sub>50</sub> values of OBP-301 in various human cancer cell lines including SCCHN cell lines (Fig. 2C), indicating that the outcome of OBP-301 treatment could be predicted by measuring GFP expression following OBP-401 infection.

**In vivo antitumor effect of intratumoral injection of OBP-301 in an orthotopic nude mouse model of human SCCHN.** To assess the effect of OBP-301 on SCCHN *in vivo*, we used an orthotopic animal model for SCCHN in which SAS-L cells were implanted into the tongues of BALB/c *nu/nu* mice. Histopathologic examination of the excised primary tumors showed a tumor formation composed of implanted SAS-L cells with a solid architecture (Fig. 3A). Mice bearing palpable SAS-L tumors with a diameter of 3 to 5 mm received three courses of intratumoral injections of  $10^8$  pfu of OBP-301 or PBS (mock treatment) every 3 days beginning on the 7th day (regimen 1) or 10th day (regimen 2) after the initial tumor inoculation (Fig. 3B). Representative images from each group showed that tumors treated with OBP-301 starting on day 7 after tumor inoculation were consistently smaller than those of mock-treated mice 28 days after the first viral injection (Fig. 3C).

Tumor growth at the primary site and body weight were continuously monitored. Intratumoral injection of OBP-301 in both regimens induced a gradual reduction in tumor volumes compared with mock-treated mice. Mice with tumor shrinkage significantly recovered body weight starting on day 10 (regimen 1) or day 15 (regimen 2) after the last virus injection ( $P < 0.05$ ), although there was a decrease in body weight in the control group (Fig. 3D). This antitumor effect could be observed in mice orthotopically implanted with HSC-3 cells; the appearance of the effect, however, was ~4 to 5 days slower than that of SAS-L tumor-bearing mice (Supplementary Fig. S4).

**Locoregional spread of virus following virotherapy in an orthotopic human SCCHN model.** SCCHN patients with metastases to regional lymph nodes have a poorer prognosis than patients without nodal metastases (16). To verify whether adenoviruses could traffic to regional lymph nodes through the lymphatics, we injected  $1 \times 10^8$  pfu of OBP-401 into SAS-L tumors implanted into the tongues of mice. Five days after virus injection, primary tongue tumors

as well as lymph node metastases could be detected as light-emitting spots with GFP fluorescence under the optical charge-coupled device imaging (Fig. 5A). We also found that OBP-401 could infect and replicate in SAS-L cells trafficking in lymphatic vessels (Fig. 5B). These results suggest that although adenoviruses could effectively drain to regional lymph nodes, OBP-401 replicated only in metastatic lymph nodes, which was confirmed by a histopathologic analysis. Metastatic SCCHN cells were mostly observed in the lymph nodes with fluorescence emission, whereas most of GFP-negative lymph nodes contained no tumor cells (Fig. 5C). The optical imaging detected 13 lymph nodes labeled in spots with GFP fluorescence in 14 metastatic nodes (sensitivity of 92.9%). Among 21 metastasis-free lymph nodes, 3 nodes were GFP positive (specificity of 85.7%). In another orthotopic model implanted with HSC-3 human SCCHN cells, we could also detect GFP signals in one or two metastatic lymph nodes but not in other nonmetastatic nodes and salivary glands (Fig. 5; Supplementary Fig. S5).

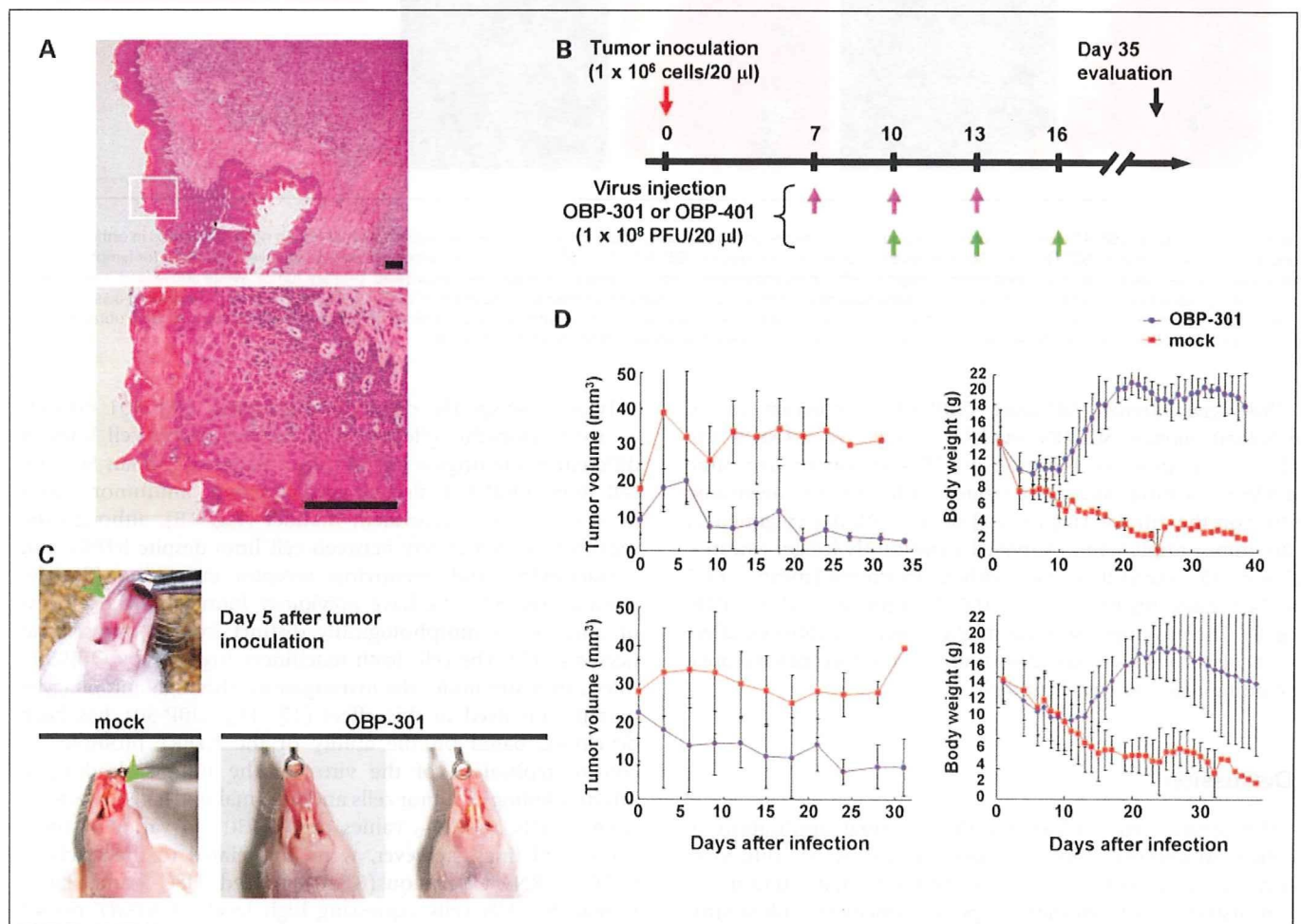


**Fig. 3.** Antitumor effects of OBP-301 *in vivo* in an orthotopic SCCHN model. **A**, tumor sections were obtained 35 d after tumor cell implantation. Paraffin-embedded sections of SAS-L tongue tumors were stained with H&E. Scale bar, 100  $\mu$ m. Top,  $\times 40$  magnification; bottom, detail of the boxed region of the top panel; magnification,  $\times 400$ . **B**, orthotopic animal experiment regimens. The tongues of BALB/c *nu/nu* mice were inoculated with  $1 \times 10^5$  SAS-L human SCCHN cells. Orthotopic tumor-bearing mice received three courses of intratumoral injection of  $1 \times 10^8$  pfu of viruses every 3 d starting on day 7 (regimen 1) or day 10 (regimen 2) after tumor cell inoculation. Eight mice were used in each group. **C**, macroscopic appearance of SAS-L tongue tumors on BALB/c *nu/nu* mice 5 d (top) or 35 d (bottom) after tumor cell inoculation. Representative tumors treated with PBS or OBP-301 are shown. Note the eradicated tumors in mice that received OBP-301 injection. Green arrowhead, SAS-L tumors. **D**, orthotopic tumor-bearing mice received three courses of intratumoral injection of  $1 \times 10^8$  pfu of viruses every 3 d starting on day 7 (regimen 1; top) or day 10 (regimen 2; bottom) after tumor cell inoculation. The tumor volume (left) and the body weight (right) were monitored and plotted. Point, mean; bars, SD. Statistical significance was defined as  $P < 0.05$ .

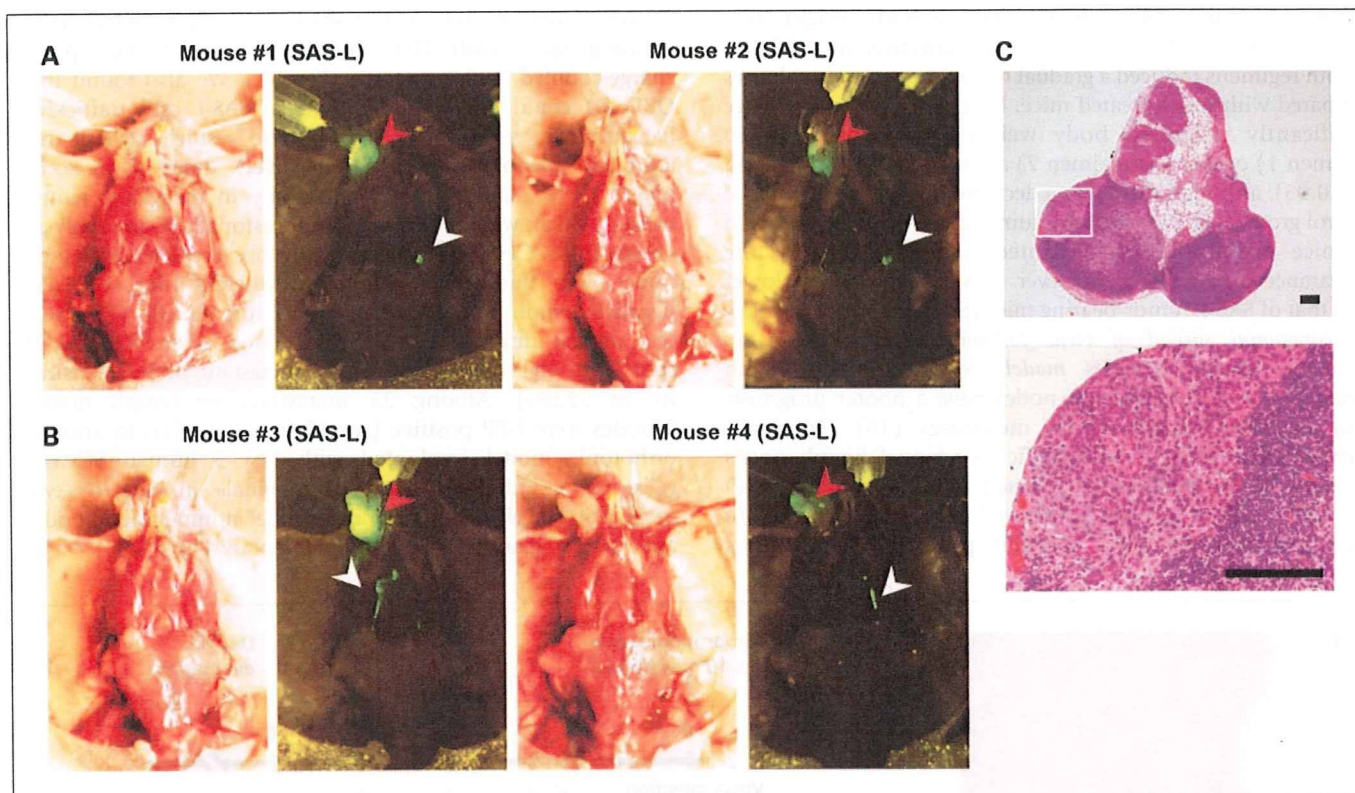


**Fig. 4.** Virus spread of OBP-401 via lymphatics to regional lymph nodes on SAS-L tumor-bearing mice. **A**, selective visualization of lymph node metastasis in orthotopic xenografts of SAS-L human SCCHN cells. Mice received intratumoral injection of OBP-401 ( $1 \times 10^8$  pfu) 24 d after tumor inoculation and were assessed for lymph node metastasis 5 d later under charge-coupled device imaging. Left, gross appearance; right, fluorescence image. Red arrowhead, primary tumor; white arrowhead, metastatic tumor cells. **B**, selective visualization of lymph node metastasis and lymphatic dissemination in orthotopic xenografts of SAS-L cells. Note the GFP-expressing disseminated tumor cells in lymphatics. Red arrowhead, primary tumor; white arrowhead, metastatic tumor cells in lymphatics. **C**, sections of GFP-positive lymph nodes were obtained 35 d after tumor cell implantation. Paraffin-embedded sections of lymph nodes were stained with H&E. Scale bar, 100  $\mu$ m.

**Prolonged survival following OBP-301 virotherapy in an orthotopic human SCCHN model.** Finally, we assessed the effect of intratumoral injection of OBP-301 on survival time of SAS-L-bearing mice. Mice treated with OBP-301 beginning either on the 7th day (regimen 1) or the 10th day (regimen 2) after tumor implantation survived significantly longer (mean = 27.4 or 33.7 days) than mice without treatment (mean = 14.7 or 24.3 days; regimen 1,  $P = 0.017$ ; regimen 2,  $P = 0.016$ ; Fig. 6). The prolonged survival might reflect an antitumor effect of oncolytic adenoviruses spreading into the locoregional area, including regional lymph nodes.

## Discussion

The present study illustrates the potential application of replication-selective oncolytic adenoviruses as an anticancer agent in human SCCHN patients. We found that intratumoral administration of telomerase-specific oncolytic adenovirus induced tumor volume reduction as well as the recovery of weight loss by enabling oral ingestion in an orthotopic xenograft model, in which human SCCHN cells were implanted into the tongues of BALB/c *nu/nu* mice. Oncolytic virotherapy also prolonged the survival of SCCHN tumor-bearing mice, presumably due to the locoregional antitumor effect against primary tumors and lymph node metastases with viruses spreading into the lymphatics.

Telomerase-specific oncolytic adenovirus OBP-301 exhibits a broad cytopathic effect against human cancer cell lines of different tissue origins (8–10). In a panel of human SCCHN cell lines, OBP-301 also showed apparent antitumor effects *in vitro* in a dose-dependent manner (Fig. 1B), although the sensitivity varied greatly between cell lines despite hTERT and coxsackievirus and adenovirus receptor expression (Supplementary Fig. S1). We have previously found that the process of oncolysis is morphologically distinct from apoptosis and necrosis (17). The cell death machinery triggered by OBP-301 infection is still under the investigation, although autophagy is partially involved in this effect (17, 18). OBP-301 has been developed based on the ability of the hTERT promoter to control replication of the virus in the tumors, leading to selective killing of tumor cells and minimal undesired effects on normal cells; the  $ID_{50}$  values of OBP-301 in various human cancer cell lines, however, were not related to the levels of hTERT mRNA expression (8, 10). Indeed, HSC-3 and HSC-4 human SCCHN cells expressing high levels of hTERT mRNA were less sensitive to OBP-301 than SCC-4 and SCC-9 cells with low levels of hTERT expression. Thus, neither hTERT expression nor coxsackievirus and adenovirus receptor expression could be useful for predicting the outcome of OBP-301 treatment.

Biomarkers have been extensively studied and often used to predict the potential therapeutic benefit of new agents, including molecular-targeted therapies (19). There is a widely recognized need for biomarkers that could improve the

clinician's ability to select suitable drugs for appropriate patients. We found that the levels of GFP expression following OBP-401 infection were highly associated with  $ID_{50}$  values of OBP-301 in individual cell lines *in vitro* (Fig. 2C). This correlation may be an expected result, because OBP-301 and OBP-401 have the same genomic backbone except for the GFP expression cassette. Although it is necessary to establish the assay procedures for GFP-based fluorescence measurement in more detail, we propose the diagnostic application of OBP-401 to predict tumor responses to OBP-301. For example, when the biopsy tissue samples of the tumor are exposed to OBP-401 for a certain amount of time *ex vivo*, the levels of GFP expression may be of value as a positive predictive marker for the outcome of OBP-301 virotherapy. Further prospective clinical studies are required to confirm the direct correlation between the GFP expression in biopsy samples following *ex vivo* OBP-401 infection and the clinical responses to OBP-301 in patients with SCCHN.

An orthotopic nude mouse model to investigate the cellular and molecular mechanisms of metastasis in human neoplasia was first described by Fidler et al. (20, 21) and Killion et al. (22). The orthotopic implantation of tumor cells restores the

correct tumor-host interactions, which do not occur when tumors are implanted in ectopic subcutaneous sites (20). To further explore the *in vivo* antitumor effects of telomerase-specific virotherapy for SCCHN, we used an orthotopic nude mouse model of human tongue squamous cell carcinoma. In our preliminary experiments, we inoculated tumor cells into the tongue of BALB/c *nu/nu* mice and confirmed the formation of tumors with a diameter of 3 to 5 mm after 5 days and the development of metastases in neck lymph nodes after 35 days. We also identified the presence of disseminated tumor cells in the regional lymph nodes at least 10 days after tumor cell implantation by using GFP-expressing SAS-L human SCCHN cells (data not shown). Intratumoral injection of OBP-301 done 7 or 10 days after tumor inoculation significantly shrunk the tongue SAS-L tumor volumes, which in turn increased the body weight of mice by enabling oral ingestion (Fig. 3D). Moreover, HSC-3 cells were relatively resistant to OBP-301 *in vitro*; intratumoral injection of OBP-301 was, however, effective for recovering the body weight in mice bearing HSC-3 tongue tumors after a long-term observation (Supplementary Fig. S4). These results suggest that although the appearance of the effect may be slower, the *in vivo* antitumor activity could be

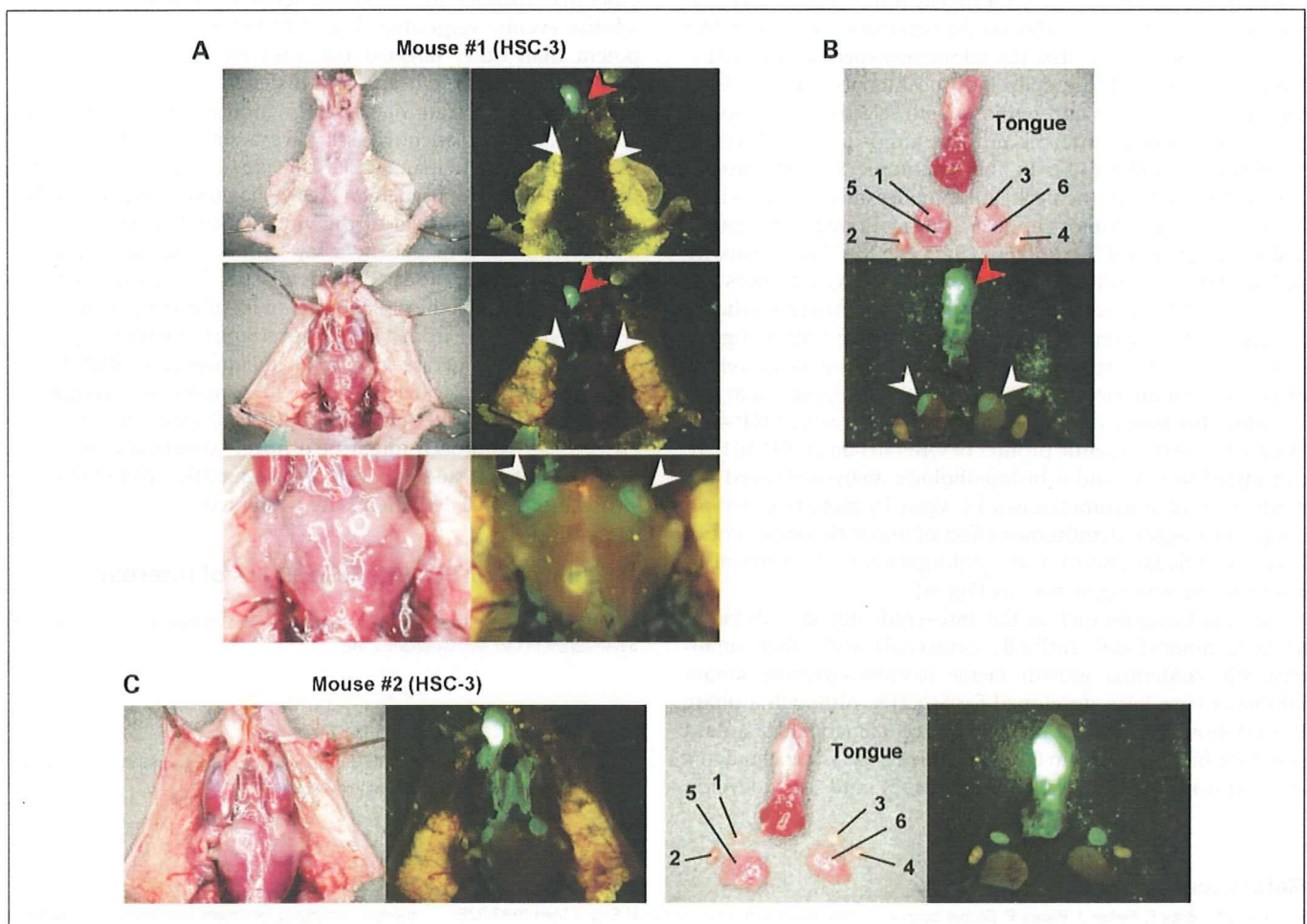


**Fig. 5.** Virus spread of OBP-401 via lymphatics to regional lymph nodes on HSC-3 tumor-bearing mice. **A**, selective visualization of lymph node metastasis in orthotopic xenografts of HSC-3 human SCCHN cells. Mice received intratumoral injection of OBP-401 at the concentration of  $1 \times 10^8$  pfu after 24 d of tumor inoculation and were assessed for lymph node metastasis 5 d later under fluorescence stereomicroscope. **B**, HSC-3 primary tumor, salivary glands, and lymph nodes were excised 5 d after OBP-401 injection and then assessed for GFP fluorescence. 1 to 4, lymph nodes; 5 and 6, salivary glands. **C**, other HSC-3 tumor-bearing mice. Excised primary tumors, salivary glands, and lymph nodes were assessed for GFP fluorescence.



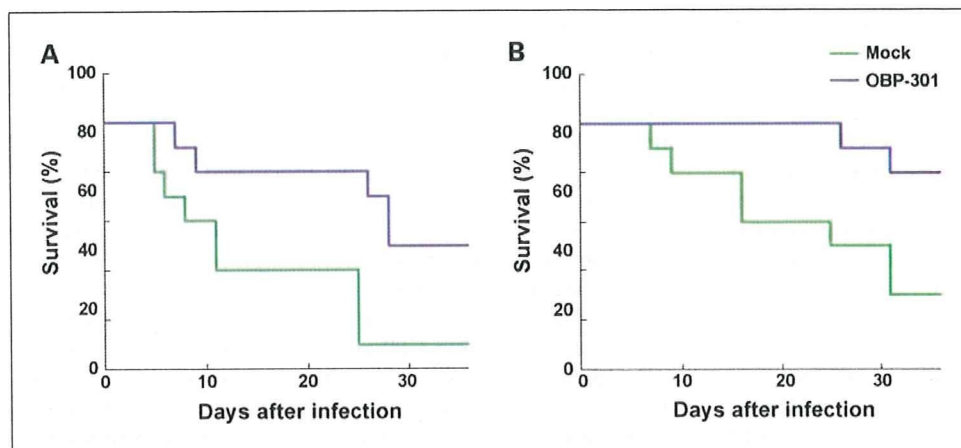


**Fig. 6.** Prolonged survival of SAS-L tumor-bearing mice treated with OBP-301. Mice bearing SAS-L xenografts were treated starting on day 7 (regimen 1; A) or day 10 (regimen 2; B) after tumor cell inoculation as described in Fig. 3A. Survival was monitored over time after virus injection and plotted as a Kaplan-Meier plot.

expected even in resistant SCCHN tumors. Because the body weight loss due to a feeding problem in this orthotopic SCCHN model resembles the disease progression in SCCHN patients, the finding that OBP-301 increased the body weight of mice suggests that OBP-301 virotherapy could potentially improve the quality of life in advanced SCCHN patients.

Amplified viruses can infect adjacent tumor cells as well as reach metastatic lymph nodes via the lymphatic circulation. We have previously shown that the telomerase-specific OBP-401-expressing GFP could be delivered into human tumor cells in regional lymph nodes and replicate with selective GFP fluorescence after injection into the primary tumor in an orthotopic rectal tumor model (11). In the orthotopic SCCHN model, OBP-401 spread into the neck lymph nodes after injection into the primary tongue tumor and selectively replicated in metastatic nodules (Figs. 4 and 5; Supplementary Fig. S5). The sensitivity and specificity of this imaging strategy for SAS-L tumors are 92.9% and 85.7%, respectively, which are sufficiently reliable to support the concept of this approach. These results suggest that surgeons may be able to excise primary tumors as well as metastatic lymph nodes precisely with appropriate margins by using this novel surgical navigation system with OBP-401. Moreover, the therapeutic profiles of OBP-401 and OBP-301 are considered similar, and a histopathologic analysis showed the destruction of micrometastases by virus in metastatic lymph nodes. This regional antitumor effect of oncolytic viruses could have a significant effect on the prolongation of the survival of mice bearing orthotopic tumors (Fig. 6).

Targeted therapies such as the anti-epidermal growth factor receptor monoclonal antibody cetuximab and other small-molecule epidermal growth factor receptor-tyrosine kinase inhibitors have been developed for SCCHN. Although a phase III trial showed a survival benefit with cetuximab and standard platinum-based therapy in SCCHN patients (23), some patients are exquisitely sensitive to these drugs and can develop

particular and severe toxicities (24). A phase I study is currently under way in the United States to determine the feasibility and to characterize the pharmacokinetics of OBP-301 in patients with histologically proven nonresectable solid tumors (25). An interim analysis of the first 12 patients, including four SCCHN patients treated with escalating doses of OBP-301, indicates that OBP-301 virotherapy is well tolerated without any severe adverse events, suggesting that OBP-301 may be much more potent than other targeted therapies for human SCCHN in terms of specificity, efficacy, and toxicity.

In conclusion, our data clearly indicate that telomerase-specific oncolytic adenoviruses have a significant therapeutic potential against human SCCHN *in vitro* and *in vivo*. Moreover, these viruses can be used in an *ex vivo* diagnostic assay to predict the therapeutic potential of the virus in SCCHN patients. The combination of a diagnostic assay with a therapeutic entity is termed theranostics (26). Telomerase-specific oncolytic viruses can be used to treat the patients and to identify the patients who will likely benefit from virotherapy (Supplementary Fig. S6). In addition, telomerase-specific *in situ* imaging strategy has a potential of being widely available in humans as a navigation system in the surgical treatment of SCCHN. Thus, our oncolytic virus-based approach might be a novel "virotheranostics" for SCCHN. Phase II studies of telomerase-specific virotheranostics in advanced SCCHN patients are warranted.

#### Disclosure of Potential Conflicts of Interest

H. Onimatsu and Y. Urata are employed by Oncolys BioPharma, Inc. T. Fujiwara is a consultant to Oncolys Biopharma, Inc.

#### Acknowledgments

We thank Daiju Ichimaru and Hitoshi Kawamura for their helpful discussions and Tomoko Sueishi for her excellent technical support.

#### References

- Parkin DM, Bray F, Ferlay J, Pisani P. Global cancer statistics, 2002. *CA Cancer J Clin* 2005;55:74–108.
- Jemal A, Clegg LX, Ward E, et al. Annual report to the nation on the status of cancer, 1975–2001, with a special feature regarding survival. *Cancer* 2004;101:3–27.
- Vokes EE, Weichselbaum RR, Lippman SM, Hong WK. Head and neck cancer. *N Engl J Med* 1993;328:184–94.
- Vokes EE, Crawford J, Bogart J, Socinski MA, Clamon G, Green MR. Concurrent chemoradiotherapy for unresectable stage III non-small cell lung cancer. *Clin Cancer Res* 2005;11:5045–50.
- Milas L, Mason KA, Liao Z, Ang KK. Chemoradiotherapy: emerging treatment improvement strategies. *Head Neck* 2003;25:152–67.
- Kirn D, Martuza RL, Zwiebel J. Replication-selective virotherapy for cancer: biological principles, risk management and future directions. *Nat Med* 2001;7:781–7.
- Hawkins LK, Lemoine NR, Kirn D. Oncolytic

- biotherapy: a novel therapeutic platform. *Lancet Oncol* 2002;3:17–26.
8. Kawashima T, Kagawa S, Kobayashi N, et al. Telomerase-specific replication-selective virotherapy for human cancer. *Clin Cancer Res* 2004;10:285–92.
  9. Taki M, Kagawa S, Nishizaki M, et al. Enhanced oncolysis by a tropism-modified telomerase-specific replication-selective adenoviral agent OBP-405 ('Telomelysin-RGD'). *Oncogene* 2005;24:3130–40.
  10. Hashimoto Y, Watanabe Y, Shirakiya Y, et al. Establishment of biological and pharmacokinetic assays of telomerase-specific replication-selective adenovirus. *Cancer Sci* 2008;99:385–90.
  11. Kishimoto H, Kojima T, Watanabe Y, et al. *In vivo* imaging of lymph node metastasis with telomerase-specific replication-selective adenovirus. *Nat Med* 2006;12:1213–9.
  12. Kotwall C, Sako K, Razack MS, Rao U, Bakamjian V, Shedd DP. Metastatic patterns in squamous cell cancer of the head and neck. *Am J Surg* 1987;154:439–42.
  13. Myers JN, Holsinger FC, Jasser SA, Bekele BN, Fidler IJ. An orthotopic nude mouse model of oral tongue squamous cell carcinoma. *Clin Cancer Res* 2002;8:293–8.
  14. Fujiwara T, Kagawa S, Kishimoto H, et al. Enhanced antitumor efficacy of telomerase-selective oncolytic adenoviral agent OBP-401 with docetaxel: preclinical evaluation of chemovirotherapy. *Int J Cancer* 2006;119:432–40.
  15. Riley T, Sontag E, Chen P, Levine A. Transcriptional control of human p53-regulated genes. *Nat Rev Mol Cell Biol* 2008;9:402–12.
  16. Lefebvre JL. Current clinical outcomes demand new treatment options for SCCHN. *Ann Oncol* 2005;16 Suppl 6:vi7–12.
  17. Endo Y, Sakai R, Ouchi M, et al. Virus-mediated oncolysis induces danger signal and stimulates cytotoxic T-lymphocyte activity via proteasome activator upregulation. *Oncogene* 2008;27:2375–81.
  18. Ito H, Aoki H, Kühnel F, et al. Autophagic cell death of malignant glioma cells induced by a conditionally replicating adenovirus. *J Natl Cancer Inst* 2006;98:625–36.
  19. Sarker D, Workman P. Pharmacodynamic biomarkers for molecular cancer therapeutics. *Adv Cancer Res* 2007;96:213–68.
  20. Fidler IJ. Rationale and methods for the use of nude mice to study the biology and therapy of human cancer metastasis. *Cancer Metastasis Rev* 1986;5:29–49.
  21. Fidler IJ, Naito S, Pathak S. Orthotopic implantation is essential for the selection, growth and metastasis of human renal cell cancer in nude mice. *Cancer Metastasis Rev* 1990;9:149–65.
  22. Killion JJ, Radinsky R, Fidler IJ. Orthotopic models are necessary to predict therapy of transplantable tumors in mice. *Cancer Metastasis Rev* 1998;17:279–84.
  23. Langer CJ. Targeted therapy in head and neck cancer: state of the art 2007 and review of clinical applications. *Cancer* 2008;112:2635–45.
  24. Widakowich C, de Castro G, Jr., de Azambuja E, Dinh P, Awada A. Review: side effects of approved molecular targeted therapies in solid cancers. *Oncologist* 2007;12:1443–55.
  25. Fujiwara T, Tanaka N, Nemunaitis J, et al. Phase I trial of intratumoral administration of OBP-301, a novel telomerase-specific oncolytic virus, in patients with advanced solid cancer: Evaluation of biodistribution and immune response. 2008 ASCO Annual Meeting Proceedings. *J Clin Oncol* 2008;26:3572.
  26. Del Vecchio S, Zannetti A, Fonti R, Pace L, Salvatore M. Nuclear imaging in cancer theranostics. *Q J Nucl Med Mol Imaging* 2007;51:152–63.

# Antiviral activity of cidofovir against telomerase-specific replication-selective oncolytic adenovirus, OBP-301 (Telomelysin)

Masaaki Ouchi · Hitoshi Kawamura · Yasuo Urata · Toshiyoshi Fujiwara

Received: 15 June 2008 / Accepted: 30 July 2008 / Published online: 27 August 2008  
© Springer Science + Business Media, LLC 2008

**Summary** We constructed a replication-competent oncolytic adenovirus, OBP-301 (Telomelysin), in which human telomerase reverse transcriptase (hTERT) promoter drives E1 genes. OBP-301 is currently being used in a phase-I clinical trial for various types of tumors. Under such conditions, anti-adenoviral agents should be available for safety use against OBP-301 since any adenoviral viremia could cause severe adverse effects. Cidofovir (CDV) is an acyclic nucleoside phosphonate that has a broad antiviral activity against DNA viruses. Here, we examined the antiviral effects of CDV against OBP-301. The *in vitro* cytopathic effects of OBP-301 were suppressed by CDV. Moreover, CDV decreased the adenoviral E1A gene copy number after OBP-301 infection. These results suggest that CDV is a potentially useful antiviral agent for OBP-301.

**Keywords** hTERT · Adenovirus · Cidofovir · Oncolytic virus · Clinical trial

## Introduction

Oncolytic adenoviruses have been developed for treatment of human cancer. These viruses are designed to replicate and selectively kill cancer cells but to have minimum effect on normal cells [1]. Two major approaches to generate selective

replication of viruses within tumor cells have been used [2, 3]. One is to delete genes that are critical for replication of the virus in normal cells but are dispensable for cancer cells such as ONYX-015 or  $\Delta 24$  [4]. The other approach is the replacement of the promoter region that initiates viral replication genes to the promoter region of the genes active in cancer cells [2, 3]. Various genetic or epigenetic targets limited to cancer cells have been investigated and used for constructing oncolytic adenoviruses.

Human telomerase reverse transcriptase (hTERT) is an enzymatic subunit of human telomerase [5]. Telomerase is expressed in almost all cancer cells but not in all normal cells [6]. Therefore, telomerase is an attractive target for treatment of cancer. We constructed previously the attenuated adenovirus, OBP-301 (Telomelysin), in which adenoviral E1A and E1B genes are linked with internal ribosomal entry site under the control of the hTERT promoter. We reported that OBP-301 induced selective expression of E1A and E1B genes in many cancer cell lines and selectively replicated and lysed cancer cells but not normal cells [7–9]. OBP-301 is currently being tested in a phase-I clinical trial that includes various types of solid tumors. Although patients receiving this type of therapy become positive for anti-adenoviral neutralizing antibodies, those treated with OBP-301 could develop adenoviral viremia with potentially severe adverse effects. Thus, there is a need for anti-adenoviral agents for treatment of potential viremia in clinical trials of OBP-301.

One of the antiviral compounds is phosphonyl acyclic nucleotides, (S)-9-(3-hydroxy-2-phosphonometoxy propyl) cytosine dehydrate, also known as HPMPC (cidofovir, or CDV). CDV was developed for the treatment of viral infections and has a broad antiviral activity against DNA viruses, such as cytomegalovirus and adenoviruses (AdV). CDV exhibits potent inhibitory effects against several

M. Ouchi · H. Kawamura · Y. Urata  
Oncolys BioPharma, Inc.,  
Tokyo 106-0032, Japan

T. Fujiwara (✉)  
Center for Gene and Cell Therapy, Okayama University Hospital,  
Okayama 700-8558, Japan  
e-mail: toshi\_f@md.okayama-u.ac.jp

adenoviral serotypes in cell culture models [10]. Furthermore, CDV has been used clinically for AdV infections after bone marrow transplantation in immunodeficient patients [11]. Thus, we presumed that CDV could be a useful antiviral drug against OBP-301. In the present study, we examined the *in vitro* inhibitory effects of CDV against OBP-301 in human lung cancer cell lines.

## Materials and methods

### Cell culture, viruses, and chemicals

The human non-small lung cancer cell H1299 and lung cancer cell line A549 were purchased from American Type Culture Collection (ATCC). H1299 was cultured in RPMI 1640 medium supplemented with 10% FCS. A549 was cultured in DMEM F12 medium supplemented with 10% fetal calf serum (FCS). OBP-301 was constructed and characterized as described previously [7–9]. The human wild-type adenovirus type 5 (wt-Ad) was also used. VISTIDE™ (CDV injection) was purchased from Gilead Sciences (Foster City, CA).

### Cell viability assay

Cells were seeded in 96-well plate at  $1 \times 10^3$  cells per well and incubated at 37°C. After incubation, cells were infected with OBP-301 at a MOI of 1 (in H1299) and 5 (in A549) for 2 hours. The medium was aspirated and replaced with fresh medium containing 2% FCS and serially diluted CDV. Cell viability was determined by XTT assay 7 days after infection using Cell Proliferation Kit II (Roche Molecular Biochemicals) according to the protocol recommended by the manufacturer. Protection was determined by the following formula: Protection (%) =  $\frac{\text{OD (AdV(+):CDV(+))} - \text{OD (AdV(+):CDV(-))}}{\text{OD (AdV(-):CDV(+))} - \text{OD (AdV(+):CDV(-))}} \times 100$ . CC<sub>50</sub> (50% cytotoxic concentration) was defined as CDV concentration that inhibited relative cell viability to 0.5 without OBP-301 infection. EC<sub>50</sub> (50% effective concentration) was defined as CDV concentration that archived 50% protection.

### Quantitative real-time PCR analysis

Cells were seeded in six-well plate at  $2 \times 10^5$  cells per well. After overnight incubation at 37°C, the medium was aspirated, and cells were infected with OBP-301 or wt-Ad at a MOI of 10 for 2 hours at 37°C with gentle shaking every 15 minutes. After incubation, the cells were washed with PBS and placed in a medium containing serially diluted CDV (100, 20, 4, 0.8, 0.16 and 0 μM). The cells were harvested 24 hours later with Trypsin/EDTA and total

DNA was extracted using QIAamp™ DNA Mini Kit (Qiagen, Hilden, Germany). Viral E1A copy number was measured using LightCycler instruments and LightCycler Faststart DNAMaster SYBR Green I (Roche, Mannheim, Germany). EC<sub>50</sub> (E1A) was defined as the CDV concentration that inhibits the E1A ratio (with CDV/no CDV) to 0.5. Primers for E1A gene were: forward: 5'- CCTGTGTCTA GAGAATGCAA -3', reverse: 5'- ACAGCTCAAGTCAAAGGTT - 3'. PCR amplification began with a 600-s of denaturation step at 95°C and then 40 cycles of denaturation at 95°C for 10 s, annealing at 60°C for 15 s, and extension at 72°C for 8 s.

### Statistical analysis

The Student's *t*-test was used to compare differences. Statistical significance was defined when *p* was <0.05.

## Results

### *In vitro* cytopathic effect of OBP-301 on lung cancer cell lines

We reported previously that OBP-301 exhibited oncolytic activity against many types of human cancer cells [7–9]. To confirm this, we tested its cytopathic effects in cancer cell line *in vitro*. Human lung cancer cell lines, A549 and H1299, were infected with OBP-301 at various MOIs and numbers of living cells were measured by XTT assay (Fig. 1). At 5 days after infection, the majority of H1299 cells were killed by OBP-301 at MOI of 1 and 10, and approximately 70% of A549 cells were killed by OBP-301 at MOI of 50. These results confirmed that OBP-301 induced cell death in A549 and H1299 cells.

### Inhibitory effects of CDV on the cytopathic effect of OBP-301

Next, we tested whether the cytopathic effect by OBP-301 on these cancer cells could be inhibited by CDV treatment. A549 and H1299 cells were infected with OBP-301 then treated with CDV at various concentrations. Cell viability was also determined by XTT assay. In the presence of the drug and virus, relative cell viability significantly increased in the presence of CDV at > 30 μM in A549 cells and > 40 μM in H1299 cells (*p*<0.01) (Fig. 2). Furthermore, inhibition of cell growth of each cell line was observed in the presence of CDV at > 100 μM. The calculated EC<sub>50</sub> values of CDV were 20.4 μM for H1299 and 35.9 μM for A549 cells, while the calculated CC<sub>50</sub> values were 146.4 μM for H1299 cells and 106.9 μM for A549 cells. Similar results were obtained by using ONYX-015 (see